ELSEVIER

Journal of Molecular Catalysis A: Chemical 101 (1995) 51–60

JOURNAL OF MOLECULAR CATALYSIS A: CHEMICAL

A quantum-chemical MINDO/3 study of methane and oxygen interactions with a pure and a modified calcium oxide surface

Nourbosyn U. Zhanpeisov [a], Volker Staemmler [b], Manfred Baerns [c,*]

[a] *Boreskov Institute of Catalysis, Novosibirsk 630090, Russia*

[b] *Lehrstuhl für Theoretische Chemie, Ruhr-Universität Bochum, D-44780 Bochum, Germany*

[c] *Lehrstuhl für Technische Chemie, Ruhr-Universität Bochum, D-44780 Bochum, Germany*

Received 30 August 1994; accepted 21 February 1995

Abstract

Within the framework of the MINDO/3 method methane and oxygen interactions with pure and modified calcium oxide have been considered. It is shown that low-coordinated Ca^{2+}_{3C}–O^{2-}_{4C} and Ca^{2+}_{4C}–O^{2-}_{3C} pairs of acid–base centers are responsible for the initial step in the methane activation on pure calcium oxide. Atomic oxygen strongly adsorbs only on surface basic sites yielding surface O_2^{2-} species. Molecular oxygen adsorbs both on acid and basic sites and forms either π-complexes or O_3 species, respectively. However, the dissociative adsorption of molecular oxygen on adjacent pairs of basic sites is energetically more favorable. The energetics of the substitution of a Ca^{2+}_{LC} ion by Mg^{2+}_{LC} in Mg/CaO, Na^{+}_{LC} in Na/CaO and Zn^{2+}_{LC} in Zn/CaO and Na/Zn/CaO and the methane activation on these modified calcium oxides have also been considered. The results allow an understanding of the experimentally observed increase of the C_{2+} hydrocarbon selectivity in the oxidative coupling of methane both on mixed magnesium and calcium oxides containing 10 to 15% of CaO and on NaOH-promoted CaO catalysts containing minor amounts of Zn^{2+} cations.

Keywords: Adsorption; Calcium oxide; Methane; Oxygen; Quantum-chemical study

1. Introduction

During the past decade the catalytic conversion of methane into more valuable C_{2+} hydrocarbon products has been the subject of numerous studies. Most of the catalyst systems used for the oxidative coupling of methane are based on alkaline earth metal oxides doped with alkali metals, rare earth metal oxides, other mixed metal oxides and metal chlorides (see for example, [1–10]). It is well-known that magnesium oxide and calcium oxide, especially when doped with lithium and sodium ions, or mixed oxides of magnesium and calcium are very effective catalysts for this reaction [2,3,5–7]. The conception of the heterogeneous–homogeneous nature of the methane oxidative coupling reaction is now beyond any doubt. However, disagreement remains regarding the identity of the surface sites on which hydrogen atom abstraction occurs and the nature of the C–H bond breaking that is involved in methyl radical formation. Though it is quite certain that the initial step in the selective oxidation of methane occurs on the surface, there remain many questions to be solved, such as the nature of the active sites and

* Corresponding author.

SSDI 1381-1169(95)00042-9

the reaction mechanism. According to earlier assumptions, methane activation occurs homolytically via H abstraction by a partially reduced surface oxygen species whereby methyl radicals are directly released into the gas phase [2,3]. According to later suggestions, C–H bond cleavage in methane occurs heterolytically on coordinatively unsaturated acid–base pair sites of the catalysts [11–13]. The presence of such low-coordinated surface atoms on the real oxide catalysts has been evidenced spectroscopically [12]. Both the relatively high values of the activation energy for methane oxidative coupling and the H–D exchange in methane, which were observed in many catalytic systems, can serve in favour of the last proposition. Nevertheless, this remained the focus of active research in catalysis by using modern experimental as well as theoretical methods. The theoretical treatment of catalytic systems can provide complementary information concerning the mechanism and the active site.

Several theoretical studies have been performed for the adsorption of small molecules on pure or modified magnesium oxide surfaces, in particular for the adsorption of H_2, CO, methane, water, O_2 and so on using ab initio, density functional and semiempirical methods (see for example [8,14–22]. In these studies it had been shown that a heterolytic dissociation occurs during hydrogen and methane adsorption on magnesium oxides. Pairs of three-coordinated surface magnesium and oxygen atoms are the most active sites for the heterolytic dissociation. To our knowledge, no detailed theoretical studies have been performed for the adsorption of these molecules, in particular of hydrogen and methane, on calcium oxide.

In the present investigation we have studied methane and oxygen interactions with pure and modified calcium oxide surfaces using a specially parametrized semiempirical MINDO/3 method. This method allows us to calculate rather reliably the equilibrium geometries and heats of formation of various surface complexes which can be used to describe the methane and oxygen chemisorption on these oxides. Furthermore, in this semiempirical framework we have the possibility of performing quantum-chemical calculations for large surface fragments of the oxide lattice. In the present paper we obtain a detailed picture of the dissociative interaction of methane and the adsorption of oxygen on calcium oxide, which can be easily compared with our analogous calculations on magnesium oxide [19–22]. On the basis of the present computational results, the methane activation is discussed on pure calcium oxide, on calcium oxide with preadsorbed oxygen, and on calcium oxide doped with sodium (Na/CaO), magnesium (Mg/CaO), zinc (Zn/CaO) and zinc/sodium (Zn/Na/CaO). The results obtained allow us to understand the experimentally observed increase of the C_{2+} hydrocarbon selectivity in the oxidative coupling of methane both on mixed magnesium and calcium oxides containing 10 to 15% of CaO and on a NaOH-promoted CaO catalyst containing minor amounts of Zn^{2+} cations.

2. Method of calculation and cluster model

The quantum-chemical cluster calculations were performed within the framework of the MINDO/3 method [23]. Restricted Hartree–Fock calculations were performed throughout; the MINDO/3 parametrization was extended for Ca-containing compounds. To optimize the necessary binding parameters α and β for core–core and core–resonance interactions between a pair of atoms in the MINDO/3 method [23] we used our automatic optimization program [24] with the procedure proposed by Dewar et al. [25]. The latter depends on a least-squares fit to the heats of formation of a set of standard molecules and to the bond lengths in those of them, for which accurate experimental data are available [25]. The so-called one-center parameters for the calcium atom were taken from [26] except for the ionization potentials of the 4s and 4p atomic orbitals (AOs) which were taken from [27]. The MINDO/3 parametrization for Na and Zn containing compounds has been performed previously; the parameters are given in [24].

Table 1
Optimized two-center parameters and for some pairs of atoms in the MINDO/3 method

Bond type	β	α
Ca–H	0.232596	0.627296
Ca–C	0.325055	0.585750
Ca–O	0.552198	1.024515
Ca–F	0.328754	1.153655
Ca–Cl	0.308864	0.835337
Ca–Ca	0.055251	0.817502

Table 1 shows the optimized binding parameters (α and β) between Ca and X atoms, where X = H, C, O, F, Cl, Ca. Table 2 compares the calculated and observed heats of formation and geometries for a set of Ca-containing compounds. As is evident, the agreement between calculated and observed data is quite good. Note in particular the good fit for CaH, $Ca(OH)_2$, CaF_2, and $CaCl_2$.

Calcium oxide which has the rock salt structure is modelled by stoichiometric clusters Ca_nO_n, where $n = 9$, 12, 18 and 32 (see Fig. 1), which contain all sorts of low-coordinated calcium and oxygen atoms in various structural defects, i.e. corners, edges, steps, etc. Table 3 and Table 4 show optimized geometries and effective Mulliken charges in dependence on the coordination number of the atoms in these clusters. For comparison the same properties are also given for a calcium oxide cube containing only four three-coordinated calcium and oxygen atoms, i.e. a Ca_4O_4 cluster. As is clear, the increase of the cluster size does not lead to essential changes in the geometry and in the charge state of similar surface regions, i.e. corners, edges, faces, etc. Only a small difference between the optimized CaO bond length at the clean (001) surface of calcium oxide and the bulk value of 0.245 nm was observed, while three-coordinated corner calcium ions show much more geometry relaxation compared to the bulk, as already observed for magnesium oxide [19]. It should be noted, that a linear correlation between the heats of formation of the clusters studied and the types of acid–base pair centers is observed; it can be expressed as follows:

$$\Delta H_f^\circ(Ca_nO_n) = -93.4m_{3C} - 146.2m_{4C} - 199.6m_{5C} - 214.4m_{6C} \quad (1)$$

Table 2
Calculated and observed heats of formation (ΔE, kcal/mol) and geometries (bond lengths in nm, bond angles in degrees) of some Ca-containing molecules and radicals [a]

Compound	ΔE	Geometry
CaH	55.5 (55.5)	CaH, 0.2012 (0.2002)
CaH_2	49.6	CaH, 0.1926; HCaH, 180
CaOH	−34.8 (−43.0 ± 3)	CaO, 0.2131; OH, 0.0940
$CaOH^+$	100.4 (87.71 ± 5)	CaO, 0.2028; OH, 0.0939
$Ca(OH)_2$	−130.9 (−130)	CaO, 0.2103 (0.21); OH, 0.0935 (0.096)
CaO	32.1 (11.2; 42.5)	CaO, 0.1966 (0.1822)
CaO^+	194.3	CaO, 0.2063
Ca(OH)F	−159.9 (−164.8 ± 5)	CaO, 0.2112; OH, 0.0935; CaF, 0.2111
Ca(OH)Cl	−120.2 (−129.0 ± 5)	CaO, 0.2100; OH, 0.0935; CaCl, 0.2483
CaC_2	169.8 (158.5 ± 10)	CaC, 0.2591 (0.2595); CC, 0.1189 (0.1191)
$Ca(CH_3)_2$	81.2	CaC, 0.2517; CH, 0.1114; HCCa, 113.2
$Ca(OH)CH_3$	−25.1	CaC, 0.2506; CaO, 0.2097; OH, 0.0936; CH, 0.1115; HCCa, 113.4; OCaC, 180
CaF	−62.9 (−65.4)	CaF, 0.2098
CaF^+	71.0	CaF, 0.2018
CaF_2	−186.6 (−186.3)	CaF, 0.2112 (0.21); FCaF, 180
CaCl	−27.3 (−22.5)	CaCl, 0.2492 (0.2439)
$CaCl_2$	−108.4 (−111.5 ± 3)	CaCl, 0.2485 (0.251); ClCaCl, 180
Ca_2Cl_4	−287.6 (−273.3)	CaCl, 0.2494; CaCl′, 0.2730; ClCaCl′, 139.4
Ca_2	82.5 (82.2)	CaCa, 0.3639 (0.4277)

[a] Available experimental data are taken from [28–30] and are given in parentheses.

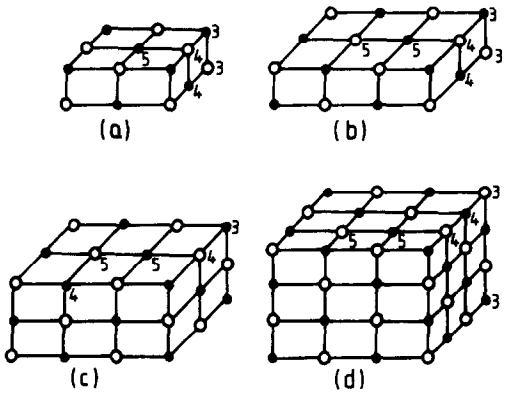

Fig. 1. Molecular clusters modelling calcium oxide surfaces: (a) Ca_9O_9, (b) $Ca_{12}O_{12}$, (c) $Ca_{18}O_{18}$, (d) $Ca_{32}O_{32}$. The numbers correspond to the degree of coordination (LC) of cations and anions: ● Ca^{2+}_{LC}, ○ O^{2-}_{LC}.

Table 3
Optimized geometries (bond length in nm) for the clusters of Ca_nO_n ($n=4, 9, 12, 18, 32$) as calculated by the MINDO/3 method

Bond type	$n=4$	$n=9$	$n=12$	$n=18$	$n=32$
Ca_{6C}–O_{6C}	–	–	–	0.2427	0.2526
Ca_{6C}–O_{5C}	–	–	–	0.2502	0.2557
Ca_{5C}–O_{6C}	–	–	–	0.2544	0.2454
Ca_{5C}–O_{5C}	–	0.2455	0.2529	–	–
Ca_{5C}–O_{5C} [a]	–	–	0.2415	0.2407	0.2383
Ca_{5C}–O_{4C}	–	0.2501	0.2499	0.2500	0.2500
Ca_{4C}–O_{5C}	–	0.2391	0.2396	0.2398	0.2396
Ca_{4C}–O_{4C}	–	0.2559	0.2556	–	–
Ca_{4C}–O_{4C} [a]	–	–	–	0.2343	0.2347
Ca_{4C}–O_{3C}	–	0.2329	0.2333	0.2333	0.2317
Ca_{3C}–O_{4C}	–	0.2279	0.2273	0.2265	0.2257
Ca_{3C}–O_{3C}	0.2295	0.2242	0.2244	–	–

[a] Second type of Ca_{LC}–O_{LC} bond in a different part of the CaO lattice.

Table 4
Effective Mulliken charges on cations and anions for the clusters of Ca_nO_n ($n=4, 9, 12, 18, 32$) as calculated by the MINDO/3 method

Type of centre	$n=4$	$n=9$	$n=12$	$n=18$	$n=32$
Ca^{2+}_{6C}	–	–	–	1.2134	1.2140
Ca^{2+}_{5C}	–	1.1324	1.1346	1.1270	1.1382
Ca^{2+}_{4C}	–	1.0541	1.0586	1.0309	1.0576
Ca^{2+}_{3C}	1.0047	1.0033	0.9952	1.0160	1.0075
O^{2-}_{6C}	–	–	–	−1.0949	−1.1267
O^{2-}_{5C}	–	−1.0192	−1.0428	−1.0512	−1.0953
O^{2-}_{4C}	–	−1.0416	−1.0500	−1.0669	−1.0973
O^{2-}_{3C}	−1.0047	−1.0442	−1.0522	−1.0734	−1.1044

where $\Delta H_f^\circ(Ca_nO_n)$ are the heats of formation of the Ca_nO_n clusters in kcal/mol; m_{3C}, m_{4C}, m_{5C}, m_{6C} is the number of three-, four-, five-, six-coordinated pairs of acid–base centers, respectively. Eq. (1) has two consequences. First, the coefficients formally correspond to the heats of formation of one CaO pair in the respective coordination state. For example, the heat of formation of one CaO pair in bulk calcium oxide is equal to −214.4 kcal/mol. Of course, these data, i.e. the heat of formation of the CaO molecule and its geometry in bulk CaO, can be easily used to reoptimize the respective binding parameters of the MINDO/3 method to study the bulk properties of calcium oxide. In this case it is also necessary to change some of the one-center one-electron parameters if one wants to correctly reproduce the charge state in bulk calcium oxide. Secondly, Eq. (1) can be applied easily to estimate the thermodynamically most stable molecular structure for larger clusters with the composition Ca_nO_n.

To study the chemisorption of methane and oxygen on calcium oxide surfaces we have preferably used a relatively large $Ca_{32}O_{32}$ cluster (Fig. 1d). To study the dissociative adsorption of methane molecule on the next-neighbour three-coordinated calcium and oxygen sites, i.e. Ca^{2+}_{3C} and O^{2-}_{3C} acid–base pairs, 'small' two-layer Ca_9O_9 and $Ca_{12}O_{12}$ clusters were used. Note, that in all calculations a full optimization of the geometry of the adsorption complexes was performed.

The calculations for the Mg/CaO, Zn/CaO, Na/CaO and Na/Zn/CaO molecular clusters were based on an isomorphic substitution of the Ca^{2+}_{LC} ion by another ion, i.e., Mg^{2+}_{LC}, Zn^{2+}_{LC}, Na^{+}_{LC}. In the sodium containing models, the resulting excess negative charge of the cluster was compensated by a proton attached to O^{2-}_{LC}. Note, the resulting clusters in all cases correspond to electroneutral closed shell states; there is no free surface valence state or an unpaired extra electron. Also for the substituted clusters, a full optimization of the local structure of the cluster was performed. There is an analogy between alkali earth metal oxides doped by alkali metals (for example, Li/MgO [19,22], Na/CaO) and acidic zeolites. The latter can be viewed as three-dimensional networks, in which only a few silicon ions are replaced by aluminum ions and protons are added

Table 5
Heats of dissociative methane adsorption (ΔE, kcal/mol) on pure calcium oxide and effective Mulliken charges on the dissociated fragments as calculated by the MINDO/3 method

Pair of centers	ΔE [a]	δq_{H^+}	$\delta q_{CH_3^-}$
Ca^{2+}_{3C}–O^{2-}_{3C}	18.7	0.2323	−0.6074
Ca^{2+}_{3C}–O^{2-}_{4C}	6.5	0.2368	−0.6578
Ca^{2+}_{4C}–O^{2-}_{3C}	6.1	0.2458	−0.6975
Ca^{2+}_{4C}–O^{2-}_{4C}	−18.6	0.2794	−0.7282
Ca^{2+}_{4C}–O^{2-}_{5C}	−27.7	0.2463	−0.6820
Ca^{2+}_{5C}–O^{2-}_{4C}	−23.5	0.2378	−0.6796
Ca^{2+}_{5C}–O^{2-}_{5C}	−38.4	0.2866	−0.7502

[a] (+) sign corresponds to stabilization of the dissociated fragments.

locally for charge compensation [31]. The protons are localized at one of the four oxygen atoms of the AlO_4^- tetrahedron forming 'bridging hydroxyl' groups and are known to be most active in the catalytic conversion of hydrocarbons [24,31].

3. Results and discussions

3.1. Adsorption of methane and oxygen on pure calcium oxide

Table 5 shows the calculated heats of dissociative methane adsorption on pure calcium oxide and the effective Mulliken charges of the dissociated fragments. These data clearly indicate that dissociative chemisorption of methane on calcium oxide proceeds not only on three-coordinated pairs of acid–base centers but also when one of the centers is four-coordinated. If one compares these results with those for magnesium oxide [19,22], one finds that the activation of methane on calcium oxide should be more favorable than on MgO. For example, the heats of dissociative adsorption of methane on Mg^{2+}_{3C}–O^{2-}_{4C} and Mg^{2+}_{4C}–O^{2-}_{3C} pairs of acid–base centers are −10.0 and −3.4 kcal/mol, respectively [19,22]. This is probably due to an increased basicity of calcium oxide as compared to magnesium oxide. The effective Mulliken charges on the basic sites can serve as a criterion for the basicity of these oxides: they are slightly higher for calcium oxide (see Table 4) than those for magnesium oxide [19]. Recent ab initio calculations on small MgO and CaO clusters have also shown that O^{2-} is more basic in CaO than in MgO [32]. Due to the very small number of next-neighbour three-coordinated pairs of acid–base centers, both Ca^{2+}_{3C}–O^{2-}_{4C} and Ca^{2+}_{4C}–O^{2-}_{3C} pairs should be responsible for the initial step in the methane activation on calcium oxide. Note, in the case of magnesium oxide only the O^{2-}_{3C}–Mg^{2+}_{4C} pair of centers is expected to be responsible for the methane activation [19,22]. The second conclusion from Table 5 is that the heterolytic dissociation leads to a noticeable polarization of the chemisorbed methane fragments; the effective charge on the methyl fragment bonded to the acid site of calcium oxide is also higher than for magnesium oxide [19].

Table 6 and Table 7 show heats of adsorption both for atomic oxygen and molecular oxygen on various active sites on pure calcium oxide, respectively. In contrast to molecular oxygen, atomic oxygen strongly adsorbs only on surface basic sites. However, in contrast to magnesium oxide, the heat of adsorption of atomic oxygen on calcium oxide increases with increasing coordination number of the active site. The values for the adsorption of atomic oxygen on magnesium oxide are equal to 73.0, 66.1 and 65.2 kcal/mol for the adsorption on three-, four-and five-coordinated basic sites, respectively. If one compares both the electronic structure and the geometry of the O_2 species formed when atomic oxygen is adsorbed on calcium oxide with free gas phase O_2^- and/or O_2^{2-} particles, one finds that the adsorbed O_2 fragment mostly resembles a O_2^{2-} species. There is no

Table 6
Heats of adsorption (ΔE, kcal/mol) of atomic oxygen on pure calcium oxide, total effective Mulliken charge on the O_2 species and its bond length (R, nm) as calculated by the MINDO/3 method [a]

Type of cluster	Type of center	ΔE	δq_{O2}	R
$Ca_{32}O_{32}$	O^{2-}_{3C}	98.8	−1.2342	0.1421
	O^{2-}_{4C}	106.4	−1.2053	0.1427
	O^{2-}_{5C}	119.4	−1.1751	0.1441

[a] The optimized bond lengths for gas phase O_2^- and O_2^{2-} are equal to 0.1308 and 0.1473 nm, respectively.

Table 7
Heats of adsorption (ΔE, kcal/mol) of molecular oxygen on pure calcium oxide, effective Mulliken charges of adsorbed oxygen and its geometry (bond lengths in nm, angles in degrees) as calculated by the MINDO/3 method using the $Ca_{32}O_{32}$ cluster

Type of center	ΔE	δq [a]	Geometry [b]
Ca^{2+}_{3C}	20.1	0.1408	CaX, 0.2489; OO, 0.1209; CaXO, 90.5; CaO, 0.2566, 0.2557
Ca^{2+}_{4C}	20.7	0.1341	CaX, 0.2515; OO, 0.1209; CaXO, 89.1; CaO, 0.2587, 0.2586
Ca^{2+}_{5C}	24.0	0.1516	CaX, 0.2506; OO, 0.1211; CaXO, 91.5; CaO, 0.2593, 0.2563
O^{2-}_{3C} [c]	43.6	−0.6074 (−1.2822)	OO′, 0.1448; O′O″, 0.1343; OO′O″, 114.6; CaO″, 0.2404
O^{2-}_{3C} [d]	84.0	−0.5769 (−1.2383)	OO′, 0.1411; O′O″, 0.1389; OO′O″, 109.4; CaO″, 0.2628
O^{2-}_{4C} [d]	81.5	−0.5843 (−1.2040)	OO′, 0.1421; O′O″, 0.1378; OO′O″, 112; CaO″, 0.2359
O^{2-}_{5C} [d]	92.1	−0.5062 (−1.1454)	OO′, 0.1450; O′O″, 0.1370; OO′O″, 113; CaO″, 0.2623

[a] Effective Mulliken charge of the adsorbed molecular oxygen, the total charge on the O_3 fragment is shown in parentheses.
[b] X is 'center of mass' of adsorbed molecular oxygen. There are two CaO bonds with similar bond lengths in the π-complex between Ca^{2+}_{LC} and O_2.
[c] The O″ atom of the adsorbed molecular oxygen forms one bond with the nearest calcium atom.
[d] The O″ atom of the adsorbed molecular oxygen forms two bonds with the two nearest calcium atoms.

O_2^- due to the lack of electron-donor defects on the calcium oxide surface studied.

Molecular oxygen can be adsorbed both on acid and basic sites. In the former case, molecular oxygen adsorbs as π-complex and its heat of adsorption slightly increases with increasing coordination number of the acid site. Note, molecular adsorption of oxygen on pure MgO leads to a stabilization of the same π-complex only in the case of participation of three-coordinated Mg^{2+}_{3C} with a heat of adsorption equal to 9.4 kcal/mol [21]. Both for MgO and CaO adsorption on basic sites is more preferable than that on acid sites and corresponds to chemisorption. The geometry of the O_3 fragment for a molecular oxygen adsorbed on a basic site strongly differs from that of an O_3^- particle in the gas phase, although the electronic distribution differs only slightly from that of the free gas-phase O_3^- species. However, this species cannot be ascribed to an adsorbed O_3^- because of the lack of an extra unpaired electron on the oxide surface. Evidently, the homolytic dissociative adsorption of molecular oxygen on a pair of O^{2-}_{LC}–O^{2-}_{LC} centers is also possible, because the heat of adsorption of atomic oxygen is slightly higher than that for molecular adsorption. For example, dissociative adsorption of molecular oxygen on next-neighbour O^{2-}_{5C}–O^{2-}_{5C} centers of the (001) surface of calcium oxide proceeds with a gain in energy of 93.9 kcal/mol.

Table 8
Heats of reaction (ΔE, kcal/mol) for reactions (2) and (3) as calculated by the MINDO/3 method

Type of center	Reaction number	ΔE [a]
O^{2-}_{5C}	2	28.5
O^{2-}_{4C}	2	26.1
O^{2-}_{3C}	2	16.0
O^{2-}_{5C}	3	1.0
O^{2-}_{4C}	3	14.6
O^{2-}_{3C}	3	21.6

[a] (+) sign means that the products are lower in energy than the reagents.

The adsorbed atomic and molecular oxygen species can be easily considered as active sites for methane activation. If one considers the overall reactions of the oxidative coupling of methane given by the Eqs. (2) and (3),

$$Ca_{32}O_{31}O_{LC}O_2 + 2CH_4 \rightarrow Ca_{32}O_{31}O_{LC}O + H_2O(g) + C_2H_6(g) \quad (2)$$

$$Ca_{32}O_{31}O_{LC}O + 2CH_4 \rightarrow Ca_{32}O_{32} + H_2O(g) + C_2H_6(g) \quad (3)$$

Table 9
Heats of reaction (ΔE, kcal/mol) of Ca^{2+}_{LC} ion substitution by Me^{2+}_{LC} ion as calculated by the MINDO/3 method (Eqs. (4) and (5))

Type of cluster	Me^{2+}_{LC}	ΔE [a]
$Ca_{32}O_{32}$	Zn^{2+}_{3C}	1.5
	Zn^{2+}_{4C}	−32.4
	Zn^{2+}_{5C}	−56.4
	Mg^{2+}_{3C}	16.2
	Mg^{2+}_{4C}	4.4
	Mg^{2+}_{5C}	0.1

[a] See footnote of Table 8.

Table 10
Heats of reaction (ΔE, kcal/mol) of Ca^{2+}_{LC} ion substitution by a Na^{+}_{LC} ion and a proton bonded to a lattice O^{2-}_{LC} ion as calculated by the MINDO/3 method (Eq. (6))

Type of cluster	Na^{+}_{LC}	O^{2-}_{LC}	ΔE [a]
Ca_9O_9	Na^{+}_{3C}	O^{2-}_{3C}	55.9
	Na^{+}_{4C}	O^{2-}_{3C}	25.6
	Na^{+}_{5C}	O^{2-}_{3C}	4.4
$Ca_{32}O_{32}$	Na^{+}_{3C}	O^{2-}_{4C}	65.6
	Na^{+}_{4C}	O^{2-}_{3C}	48.0
	Na^{+}_{3C} [b]	O^{2-}_{3C}	47.0
	Na^{+}_{6C}	O^{2-}_{3C}	27.6
	Na^{+}_{4C}	O^{2-}_{4C}	24.5
	Na^{+}_{5C}	O^{2-}_{3C}	18.8
	Na^{+}_{5C}	O^{2-}_{4C}	2.5

[a] (+) sign corresponds to exothermicity of an overall reaction.
[b] Substitution of bulk Ca^{2+} ion by Na^{+} ion.

one finds that these processes are energetically favorable (Table 8). Note, the heats of reaction are calculated as energy differences between the sum of the product energies and the sum of the reagent energies. More complete MINDO/3 searches of the interaction of methane molecules with calcium oxide surfaces containing preadsorbed atomic or molecular oxygen will be performed in a later study.

3.2. Substitution of a calcium cation by other cations

The Table 9 and Table 10 Table 11 show the energetics of the substitution of one Ca^{2+}_{LC} ion by Mg^{2+}_{LC} in Mg/CaO, Na^{+}_{LC} in Na/CaO and Zn^{2+}_{LC} in Zn/CaO and Na/Zn/CaO clusters. In the cases of Na/CaO and Na/Zn/CaO the charge neutrality is achieved by adding one proton bonded to a basic surface oxygen atom. These heats of reaction are calculated using the respective overall reactions given by Eqs. (4)–(7) and are based on energy differences between the products and reagents.

$$Ca_{32}O_{32} + Zn(OH)_2 \rightarrow Ca_{31}ZnO_{32} + Ca(OH)_2 \quad (4)$$

$$Ca_{32}O_{32} + Mg(OH)_2 \rightarrow Ca_{31}MgO_{32} + Ca(OH)_2 \quad (5)$$

$$Ca_{32}O_{32} + NaOH + H_2O \rightarrow Ca_{31}NaO_{32}H + Ca(OH)_2 \quad (6)$$

$$Ca_{31}NaO_{32}H + Zn(OH)_2 \rightarrow Ca_{30}ZnNaO_{32}H + Ca(OH)_2 \quad (7)$$

Eq. (7) corresponds to the successive substitution of two Ca^{2+}_{LC} ions by sodium and zinc ions. The data in the clearly indicate that only small amounts of Ca^{2+} cations can be exchanged by Zn^{2+} in the Zn/CaO and Na/Zn/CaO clusters. In fact, only the substitution of a three-coordinated Ca^{2+} ion by a Zn^{2+} ion is energetically favorable. The same picture has been already observed for Zn/MgO and Na/Zn/MgO systems [33]. The

Table 11
Heats of reaction (ΔE, kcal/mol) of Ca^{2+}_{LC} ion substitution by Zn^{2+}_{LC} ion on calcium oxide with a presubstituted Ca^{2+}_{LC} ion by Na^{+}_{LC} ion and a proton bonded to a lattice O^{2-}_{LC} ion as calculated by the MINDO/3 method (Eq. (7))

Type of cluster	Zn^{2+}_{LC}	Na^{+}_{LC}	O^{2-}_{LC}	ΔE [a]
$Ca_{32}O_{32}$	Zn^{2+}_{3C}	Na^{+}_{4C}	O^{2-}_{4C}	−1.7
	Zn^{2+}_{4C}	Na^{+}_{3C}	O^{2-}_{3C}	−6.1
	Zn^{2+}_{3C}	Na^{+}_{3C}	O^{2-}_{3C}	−7.7
	Zn^{2+}_{4C}	Na^{+}_{3C}	O^{2-}_{3C}	−8.6
	Zn^{2+}_{3C}	Na^{+}_{5C}	O^{2-}_{3C}	−32.9
	Zn^{2+}_{3C}	Na^{+}_{4C}	O^{2-}_{4C}	−38.5
	Zn^{2+}_{3C}	Na^{+}_{5C}	O^{2-}_{4C}	−39.6
	Zn^{2+}_{4C}	Na^{+}_{4C}	O^{2-}_{3C}	−42.8
	Zn^{2+}_{5C}	Na^{+}_{3C}	O^{2-}_{4C}	−58.1
	Zn^{2+}_{5C}	Na^{+}_{3C}	O^{2-}_{3C}	−78.1

[a] See footnote of Table 10.

Table 12
Heats of dissociative adsorption of methane (ΔE, kcal/mol) on Na-promoted calcium oxide as calculated by the MINDO/3 method

Type of cluster	Na^+_{LC}	O^{2-}_{LC}	Pair of centers	ΔE [a]
$Ca_{31}NaO_{32}H$	Na^+_{3C}	O^{2-}_{3C}	Ca^{2+}_{4C}–O^{2-}_{4C}	14.4
	Na^+_{3C}	O^{2-}_{3C}	Ca^{2+}_{4C}–O^{2-}_{5C}	−28.1
	Na^+_{3C}	O^{2-}_{3C}	Ca^{2+}_{5C}–O^{2-}_{4C}	−7.5
	Na^+_{4C}	O^{2-}_{3C}	Ca^{2+}_{3C}–O^{2-}_{4C}	12.4
	Na^+_{4C}	O^{2-}_{3C}	Ca^{2+}_{5C}–O^{2-}_{4C}	−28.8
	Na^+_{4C}	O^{2-}_{3C}	Ca^{2+}_{4C}–O^{2-}_{5C}	−30.4

[a] See footnote of Table 8.

main physical reason for this is the different crystal structures of these oxides: magnesium and calcium oxides have rock salt structure, while zinc oxide forms wurtzite-type structure. That is why magnesium oxide and calcium oxide easily form mixed oxides [5,7].

Since the lattice parameters of MgO ($a=0.420$ nm [34]) and ZnO ($a=0.325$ nm, the Zn–Zn or O–O distance in the zinc-or oxygen-terminated layer [34]) are much smaller than that of CaO oxide ($a=0.490$ nm [34]) the substitution of Ca^{2+}_{LC} by these ions leads to a shortening of the respective Me–O bond lengths in the Mg/CaO and Zn/CaO clusters. For example, magnesium and zinc ions are moved by 0.0524 and 0.0560 nm in the bulk direction when a three-coordinated Ca^{2+}_{3C} ion is substituted by Mg^{2+}_{3C} or by Zn^{2+}_{3C}, respectively. This picture is much more pronounced when a Ca^{2+}_{3C} ion is substituted by Na^+_{3C} ion; the respective relaxation is equal to 0.1338 nm. It should be also noted, that the formation of a hydroxyl group on the oxygen atom next-neighbour to the sodium atom stabilizes the resulting cluster very much when a Ca^{2+}_{LC} ion is substituted by Na^+_{LC} and proton. For example, the substitution of Ca^{2+}_{3C} ion by Na^+_{3C} and a proton bonded to O^{2-}_{3C} is the most favorable case for the Ca_9O_9 cluster, however for the $Ca_{32}O_{32}$ cluster the proton is preferably bonded to the next four-coordinated basic oxygen atom (see Table 9). Similar conclusions have been drawn for zeolites [31] and for magnesium oxide when the dissociative adsorption of hydrogen was considered [14] (b), [19]. In the latter case, the dissociative adsorption of hydrogen on next-neighbour acid–base sites leads to mutual stabilization of the adsorbed fragments.

3.3. Dissociative adsorption of methane on modified calcium oxide

The Table 12 and Table 13 show heats of dissociative adsorption of methane on modified calcium oxide, i.e. on Na/CaO, Zn/CaO, Mg/CaO and Na/Zn/CaO. For comparison, analogous data for Ca/MgO oxide are also shown, where one Mg ion is substituted by one Ca ion, i.e. in a $Mg_{31}CaO_{32}$ molecular cluster. These results clearly indicate that the dissociative chemisorption of methane is enhanced when pure calcium oxide is simultaneously promoted by Na^+ and Zn^{2+} cations. For example, the activation of the methane molecule by dissociative chemisorption on a Zn^{2+}_{LC}–O^{2-}_{LC} pair of acid–base centers of Na/Zn/CaO is energetically more favorable than that on both pure CaO, ZnO [33] and Na/CaO. Furthermore, the heterolytic dissociation of the meth-

Table 13
Heats of dissociative adsorption of methane (ΔE, kcal/mol) on modified calcium oxide as calculated by the MINDO/3 method

Type of cluster	Na^+_{LC}	O^{2-}_{LC}	Me^{2+}_{LC}	Pair of centers	ΔE [a]
$Ca_{32}O_{32}$	–	–	Mg^{2+}_{3C}	Ca^{2+}_{4C}–O^{2-}_{3C}	5.3
	–	–	Mg^{2+}_{3C}	Mg^{2+}_{3C}–O^{2-}_{4C}	6.7
	–	–	Mg^{2+}_{3C}	Ca^{2+}_{3C}–O^{2-}_{4C}	5.7
	–	–	Mg^{2+}_{4C}	Mg^{2+}_{4C}–O^{2-}_{3C}	6.1
	–	–	Mg^{2+}_{5C}	Mg^{2+}_{5C}–O^{2-}_{4C}	−29.4
$Mg_{32}O_{32}$	–	–	Ca^{2+}_{4C}	Ca^{2+}_{4C}–O^{2-}_{3C}	7.4 [b]
	–	–	Ca^{2+}_{3C}	Ca^{2+}_{3C}–O^{2-}_{4C}	7.8 [b]
$Ca_{32}O_{32}$	–	–	Zn^{2+}_{3C}	Zn^{2+}_{3C}–O^{2-}_{4C}	14.1
	–	–	Zn^{2+}_{4C}	Zn^{2+}_{4C}–O^{2-}_{3C}	17.5
	Na^+_{4C}	O^{2-}_{3C}	Zn^{2+}_{3C}	Zn^{2+}_{3C}–O^{2-}_{4C}	31.7
	Na^+_{3C}	O^{2-}_{4C}	Zn^{2+}_{3C}	Zn^{2+}_{3C}–O^{2-}_{4C}	16.8
	Na^+_{3C}	O^{2-}_{4C}	Zn^{2+}_{4C}	Zn^{2+}_{4C}–O^{2-}_{3C}	21.2
	Na^+_{3C}	O^{2-}_{4C}	Zn^{2+}_{3C}	Ca^{2+}_{4C}–O^{2-}_{4C}	−4.9
	Na^+_{3C}	O^{2-}_{4C}	Zn^{2+}_{4C}	Zn^{2+}_{4C}–O^{2-}_{4C}	15.2
	Na^+_{3C}	O^{2-}_{4C}	Zn^{2+}_{4C}	Zn^{2+}_{4C}–O^{2-}_{5C}	−6.0

[a] See footnote of Table 8.

[b] These values correspond to modified magnesium oxide in which one Mg^{2+}_{LC} ion is substituted by one Ca^{2+}_{LC}. If one compares these values with those for pure magnesium oxide [19] one finds that methane activation on modified magnesium oxide is energetically more favorable than on pure magnesium oxide.

ane molecule leads to a noticeable polarization of the chemisorbed fragments; however, the effective charge on the methyl fragment bound to a zinc ion of Na/Zn/CaO is only −0.229, i.e. much smaller than if it is bound to a calcium ion (−0.638). The effective Mulliken charges on the sodium and zinc atoms of Na/Zn/CaO virtually coincide with those on the lithium and zinc atoms of Li/Zn/MgO [33]. The dissociative chemisorption of the methane molecule on a Ca^{2+}_{LC}–O^{2-}_{LC} pair of centers is more favorable than on a Mg^{2+}_{LC}–O^{2-}_{LC} pair of Ca/MgO, while the substitution of Ca^{2+}_{LC} ion by Mg^{2+}_{LC} ion leads only to comparable activity of Mg^{2+}_{LC}–O^{2-}_{LC} and Ca^{2+}_{LC}–O^{2-}_{LC} pairs of centers of Mg/CaO.

These results allow us to interpret the available experimental data [5,7,35]. First, mixed magnesium and calcium oxides that contain 10 to 15% of CaO exhibit extraordinarily high activities and selectivities for C_{2+} hydrocarbon formation [5,7]. Secondly, the C_{2+} hydrocarbon selectivity increases in the oxidative coupling of methane when a NaOH-promoted CaO catalyst contains minor amounts of Zn^{2+} cations [35]. The decrease in selectivity of the latter catalyst at higher zinc oxide concentrations is probably due to the formation of ZnO clusters on the calcium oxide surface, which favors non-selective methane conversion, as explained for Li/Zn/MgO [33].

The heterolytic adsorption of methane on these oxides corresponds only to the initial step of the oxidative coupling of methane. However, the increase of the number of pairs of active acid–base sites which are able to dissociate methane leads also to an increase of methyl radicals in the gas phase. The idea is that the energy necessary for the desorption of a methyl radical into the gas phase corresponds to the activation energy for this reaction. The binding energies of the methyl group with the Lewis acid site of these oxides are essentially lower than that of the C–H bond in the methane molecule.

4. Conclusions

The numerical results of the present MINDO/3 study of the adsorption of oxygen and methane on pure and modified calcium oxide surfaces which are represented by different Ca_nO_n clusters can be summarized as follows:

(a) The initial step in methane activation on pure CaO is a heterolytic dissociation of methane on Ca^{2+}_{3C}–O^{2-}_{4C} and Ca^{2+}_{4C}–O^{2-}_{3C} pairs of low-coordinated acid–base centres. The dissociative adsorption of methane is more favourable on CaO than on MgO.

(b) Atomic oxygen adsorbs on the basic sites of a pure CaO surface yielding O^{2-}_2 species while molecular oxygen can be adsorbed both on basic and acid sites forming either π-complexes or O^{2-}_3 species. However, the homolytic dissociation of O_2 and the subsequent adsorption of the two atoms on adjacent O^{2-}_{5C} centres is energetically more favourable.

(c) The substitution of one low-coordinated Ca^{2+} ion by one Mg^{2+}, Na^+ or Zn^{2+} ion leads to considerable changes in the local geometric structure around the impurity ion. Only three-coordinated Ca^{2+} ions can be replaced by Zn^{2+} while the replacement of higher-coordinated Ca^{2+} ions by Zn^{2+} is energetically very unfavourable. On the other hand, energy is gained when three- and four-coordinated Ca^{2+} ions are substituted by Mg^{2+} while the replacement of higher coordinated Ca^{2+} is nearly thermoneutral, probably because CaO and MgO have similar crystal structures.

(d) The dissociative adsorption of methane on magnesium oxide is slightly facilitated by low-coordinated Ca^{2+} impurities. On the other hand, no noticeable stabilization can be obtained if low-coordinated Ca^{2+} ions are substituted in CaO by Mg^{2+} ions. However, the dissociative adsorption of methane on CaO is largely stabilized by Zn^{2+} doping and even more if Ca^{2+} ions are replaced simultaneously by Na^+ and Zn^{2+} ions. This is in accord with experimental observations that mixed magnesium/calcium oxides with 10 to 15% of CaO show high methane-conversions activity and

that the C_{2+} hydrocarbons selectivity of CaO is increased on promoting CaO by NaOH and minor amounts of Zn^{2+} cations.

Acknowledgements

This work was supported by Deutsche Forschungsgemeinschaft (Graduiertenkolleg 'Dynamic Processes on Solid Surfaces'). N.U.Z. thanks DFG for supporting his stay at the Ruhr-Universität Bochum.

References

[1] Y. Amenomiya, V.I. Birss, M. Goledzinowski, J. Galuszka and A.R. Sanger, Catal. Rev.-Sci. Eng., 32 (1990) 163.
[2] T. Ito, J.X. Wang, C.H. Lin and J.H. Lunsford, J. Am. Chem. Soc., 107 (1985) 5062.
[3] P.G. Hinson, A. Clearfield and J.H. Lunsford, J. Chem. Soc., Chem. Commun. (1991) 430.
[4] K. Otsuka, M. Hatano and T. Komatsu, Catal. Today, 4 (1989) 409
[5] R. Philipp and K. Fujimoto, J. Phys. Chem., 96 (1992) 9035.
[6] J.A.S.P. Carreiro and M. Baerns, J. Catal., 117 (1989) 258.
[7] R. Philipp, K. Omata, A. Aoki and K. Fujimoto, J. Catal., 134 (1992) 422.
[8] T. Ito, T. Tashiro, M. Kawasaki, T. Watanabe, K. Toi and H. Kobayashi, J. Phys. Chem., 95 (1991) 4476.
[9] O.V. Buyevskaya, M. Rothaemel, H.W. Zanthoff and M. Baerns, J. Catal., 146 (1994) 346
[10] V.R. Choudhary, V.H. Rane and R.V. Gadre, J. Catal., 145 (1994) 300.
[11] E. Garrone, F.S. Stone, J. Chem. Soc., Faraday Trans. 1, 83 (1987) 1237.
[12] F.S. Stone, E. Garrone and A. Zecchina, Mater. Chem. Phys., 13 (1985) 331.
[13] V.D. Sokolovski, React. Kinet. Catal. Lett., 35 (1987) 337.
[14] (a) H. Kobayashi, M. Yamaguchi and T. Ito, J. Phys. Chem., 94 (1990) 7206. (b) H. Kobayashi, D.R. Salahub and T. Ito, J. Phys. Chem., 98 (1994) 5487.
[15] S.P. Mechandru, A.B. Anderson and J.F.J. Brazdil, J. Am. Chem. Soc., 110 (1988) 1715.
[16] (a) K. Sawabe, N. Koga, K. Morokuma and Y. Iwasawa, J. Chem. Phys., 97 (1992) 6871. (b) K. Sawabe, N. Koga, K. Morokuma and Y. Iwasawa, J. Chem. Phys., 101 (1994) 4819.
[17] G. Pacchioni, G. Cogliandro and P.S. Bagus, Int. J. Quant. Chem., 42 (1992) 1115.
[18] K. Jug, G. Geudtner and T. Bredow, J. Mol. Catal., 82 (1993) 171.
[19] N.U. Zhanpeisov, A.G. Pelmenschikov and G.M. Zhidomirov, Kinet. Catal., 31 (1990) 563 (Translated by Plenum).
[20] N.U. Zhanpeisov, A.G. Pelmenschikov and G.M. Zhidomirov, Mendeleev Commun. (1992) 148.
[21] N.U. Zhanpeisov and G.M. Zhidomirov, Mendeleev Commun. (1992) 111.
[22] N.U. Zhanpeisov and G.M. Zhidomirov, Catal. Today, 13 (1992) 517.
[23] R.C. Bingham, M.J.S. Dewar and D.H. Lo, J. Am. Chem. Soc., 97 (1975) 1275
[24] (a) G.M. Zhidomirov, A.G. Pelmenschikov, N.U. Zhanpeisov and A.G. Grebenyuk, Kinet. Catal., 28 (1987) 86. (Translated by Plenum). (b) N.U. Zhanpeisov, G.M. Zhidomirov and M. Baerns, Zh. Strukt. Khim., 35 (1994) 12 (Translated by Plenum).
[25] M.J.S. Dewar and E. Haselbach, J. Am. Chem. Soc., 92 (1970) 590
[26] A.A. Bliznyuk and A.A. Voityuk, Zh. Strukt. Khim., 29 (1988) 156. (Translated by Plenum).
[27] A.A. Radzig and B.M. Smirnov, Handbook on Atomic and Molecular Physics, Atomizdat, Moscow, 1980.
[28] K.P. Huber and G. Herzberg, Molecular Spectra and Molecular Structure, Vol. IV, Constants of Diatomic Molecules, Van Nostrand Reinhold Co., New York, 1979.
[29] K.C. Krasnov, Molecular Constants of Inorganic Compounds. Handbook, Chemistry, Leningrad, 1979.
[30] M.X. Karapetyans and M.L. Karapetyans, Basic Thermodynamic Constants of Inorganic and Organic Compounds, Chemistry, Moscow, 1968.
[31] J. Sauer, Nature (London), 363 (1993) 493.
[32] G. Pacchioni, J.M. Ricart and F. Illas, J. Am. Chem. Soc., 116 (1994) 10152.
[33] N.U. Zhanpeisov and M. Baerns, J. Mol. Catal. in press.
[34] R.W.G. Wykoff, Crystal Structures. Vol. 1, Interscience Publ., New York, 1963.
[35] T. Grzybek and M. Baerns, Appl. Catal. A, 118 (1994) 103.